MHD turbulence in the solar corona and solar wind

Pablo Dmitruk

Departamento de Física, FCEN, Universidad de Buenos Aires

Turbulence, magnetic reconnection, particle acceleration

- Understand the mechanisms that accelerate charged particles in turbulent plasmas.

Turbulence, magnetic reconnection, particle acceleration

- Understand the mechanisms that accelerate charged particles in turbulent plasmas.
- Relation to magnetic reconnection.

Turbulence, magnetic reconnection, particle acceleration

- Understand the mechanisms that accelerate charged particles in turbulent plasmas.
- Relation to magnetic reconnection.
- Clues for dissipation mechanisms.

Turbulence, magnetic reconnection, particle acceleration

- Understand the mechanisms that accelerate charged particles in turbulent plasmas.
- Relation to magnetic reconnection.
- Clues for dissipation mechanisms.
- Differential energization: $T^e_\parallel \gg T^e_\perp, \quad T^i_\perp \gg T^i_\parallel$

Turbulence, magnetic reconnection, particle acceleration

- Understand the mechanisms that accelerate charged particles in turbulent plasmas.
- Relation to magnetic reconnection.
- Clues for dissipation mechanisms.
- Differential energization: $T_{\parallel}^{e} \gg T_{\perp}^{e}, \quad T_{\perp}^{i} \gg T_{\parallel}^{i}$
- **Direct approach**: *Test particles trajectories are followed in the turbulent fields obtained from a direct numerical solution of the MHD equations.*

Dmitruk, Matthaeus, Seenu, ApJ 617, 667 (2004)
Dmitruk, Matthaeus, Seenu, Brown, ApJ 597, L81 (2003)
Ambrosiano, Matthaeus, Goldstein, Plante, JGR 93, 14383 (1988)

Advantages

- **Turbulent fields are not modeled** but a direct result of the MHD simulations: $\rightarrow$ energy cascade, coherent structures

Advantages

- **Turbulent fields are not modeled** but a direct result of the MHD simulations: $\rightarrow$ energy cascade, coherent structures
- Current sheets (reconnection) are a natural result of the (resistive) MHD evolution (i.e. **not set up as an initial condition**)

Advantages

- **Turbulent fields are not modeled** but a direct result of the MHD simulations: $\longrightarrow$ energy cascade, coherent structures
- Current sheets (reconnection) are a natural result of the (resistive) MHD evolution (i.e. **not set up as an initial condition**)

Disadvantages

- Extremely computationally demanding if we want to fully resolve from turbulent (MHD) to particle scales

Advantages

- **Turbulent fields are not modeled** but a direct result of the MHD simulations: $\rightarrow$ energy cascade, coherent structures
- Current sheets (reconnection) are a natural result of the (resistive) MHD evolution (i.e. **not set up as an initial condition**)

Disadvantages

- Extremely computationally demanding if we want to fully resolve from turbulent (MHD) to particle scales
- Lack of self-consistency in the MHD-kinetic physics interplay at the "dissipative scales"

MHD Simulations

We use turbulent fields obtained from a Direct Numerical Solution (pseudospectral code) of the **compressible 3D MHD** equations

MHD Simulations

We use turbulent fields obtained from a Direct Numerical Solution (pseudospectral code) of the **compressible 3D MHD** equations $\rightarrow \mathbf{b}(x, y, z, t), \mathbf{v}(x, y, z, t)$ fluctuating fields, with a background magnetic field $B_0\hat{\mathbf{z}}$, such that $\mathbf{B} = B_0\hat{\mathbf{z}} + \mathbf{b}$ and we set $B_0 = 8\ \delta B$, $\delta B = \langle \mid \mathbf{b} \mid^2 \rangle^{1/2}$.

MHD Simulations

We use turbulent fields obtained from a Direct Numerical Solution (pseudospectral code) of the **compressible 3D MHD** equations $\rightarrow \mathbf{b}(x, y, z, t), \mathbf{v}(x, y, z, t)$ fluctuating fields, with a background magnetic field $B_0\hat{\mathbf{z}}$, such that $\mathbf{B} = B_0\hat{\mathbf{z}} + \mathbf{b}$ and we set $B_0 = 8\ \delta B$, $\delta B = \langle |\ \mathbf{b}\ |^2\rangle^{1/2}$.

Start with some initially large scale eddies: energy containing scale (turbulent correlation length) $L = 1/2\pi$ box size.
Periodic boundary conditions.

MHD Simulations

We use turbulent fields obtained from a Direct Numerical Solution (pseudospectral code) of the **compressible 3D MHD** equations $\rightarrow \mathbf{b}(x,y,z,t), \mathbf{v}(x,y,z,t)$ fluctuating fields, with a background magnetic field $B_0\hat{\mathbf{z}}$, such that $\mathbf{B} = B_0\hat{\mathbf{z}} + \mathbf{b}$ and we set $B_0 = 8\ \delta B$, $\delta B = \langle \mid \mathbf{b} \mid^2 \rangle^{1/2}$.

Start with some initially large scale eddies: energy containing scale (turbulent correlation length) $L = 1/2\pi$ box size.
Periodic boundary conditions.

Set $\langle \mid \mathbf{v} \mid^2 \rangle^{1/2} = v_0 = \delta B/\sqrt{4\pi\rho}$ the plasma alfvenic speed based on the fluctuations (distinct from $v_A = B_0/\sqrt{4\pi\rho}$ the alfvenic speed based on the DC field, $v_A = 10 v_0$).
Plasma $\beta = v_T^2/v_A^2 = 0.16 \rightarrow v_T = 4v_0$, Mach number $M_s = v_0/c_s = 0.25$

MHD Simulations

We use turbulent fields obtained from a Direct Numerical Solution (pseudospectral code) of the **compressible 3D MHD** equations $\rightarrow \mathbf{b}(x, y, z, t), \mathbf{v}(x, y, z, t)$ fluctuating fields, with a background magnetic field $B_0\hat{\mathbf{z}}$, such that $\mathbf{B} = B_0\hat{\mathbf{z}} + \mathbf{b}$ and we set $B_0 = 8\ \delta B$, $\delta B = \langle \mid \mathbf{b} \mid^2 \rangle^{1/2}$.

Start with some initially large scale eddies: energy containing scale (turbulent correlation length) $L = 1/2\pi$ box size.
Periodic boundary conditions.

Set $\langle \mid \mathbf{v} \mid^2 \rangle^{1/2} = v_0 = \delta B/\sqrt{4\pi\rho}$ the plasma alfvenic speed based on the fluctuations (distinct from $v_A = B_0/\sqrt{4\pi\rho}$ the alfvenic speed based on the DC field, $v_A = 10 v_0$).
Plasma $\beta = v_T^2/v_A^2 = 0.16 \rightarrow v_T = 4v_0$, Mach number $M_s = v_0/c_s = 0.25$

Reynolds numbers $R = v_0 L/\nu = R_m = v_0 L/\mu = 1000$ (limited by numerical resolution at 256^3)

MHD Simulations

We use turbulent fields obtained from a Direct Numerical Solution (pseudospectral code) of the **compressible 3D MHD** equations $\rightarrow \mathbf{b}(x,y,z,t), \mathbf{v}(x,y,z,t)$ fluctuating fields, with a background magnetic field $B_0\hat{\mathbf{z}}$, such that $\mathbf{B} = B_0\hat{\mathbf{z}} + \mathbf{b}$ and we set $B_0 = 8\ \delta B$, $\delta B = \langle \mid \mathbf{b} \mid^2 \rangle^{1/2}$.

Start with some initially large scale eddies: energy containing scale (turbulent correlation length) $L = 1/2\pi$ box size.
Periodic boundary conditions.

Set $\langle \mid \mathbf{v} \mid^2 \rangle^{1/2} = v_0 = \delta B/\sqrt{4\pi\rho}$ the plasma alfvenic speed based on the fluctuations (distinct from $v_A = B_0/\sqrt{4\pi\rho}$ the alfvenic speed based on the DC field, $v_A = 10v_0$).
Plasma $\beta = v_T^2/v_A^2 = 0.16 \rightarrow v_T = 4v_0$, Mach number $M_s = v_0/c_s = 0.25$

Reynolds numbers $R = v_0 L/\nu = R_m = v_0 L/\mu = 1000$ (limited by numerical resolution at 256^3)

Run the code for two $t_0 = L/v_0$ (eddy turnover times), fully turbulent state developed, take a **snapshot** for pushing the test particles.

MHD turbulence energy spectrum: obtained

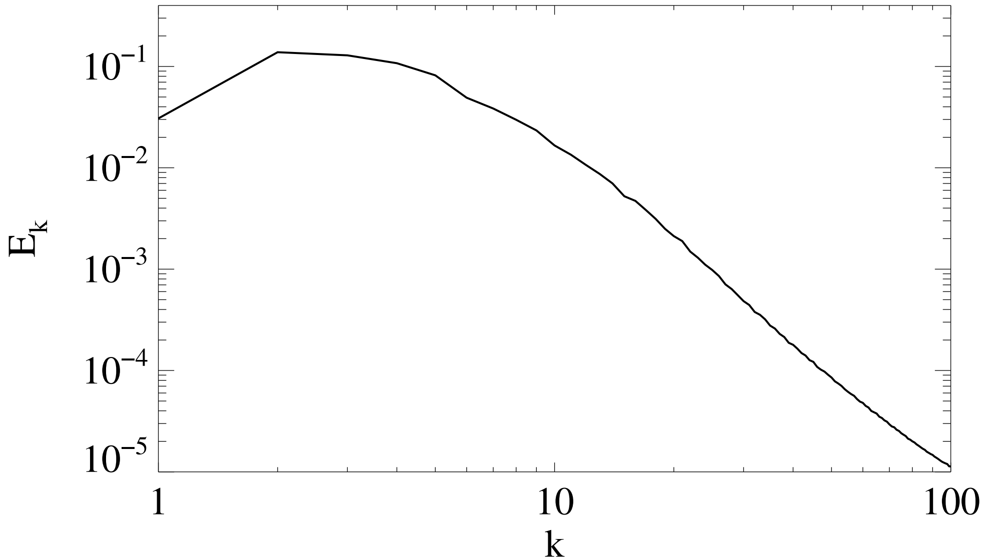

MHD spatial structure: parallel current density J_z

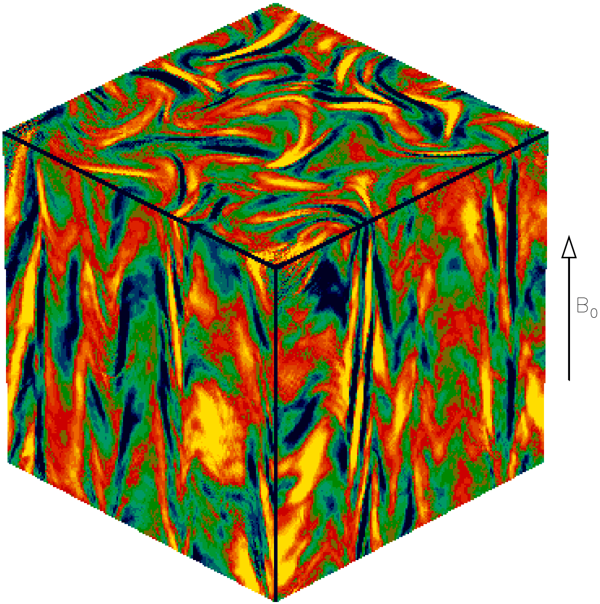

Cross-sections: magnetic field over current density

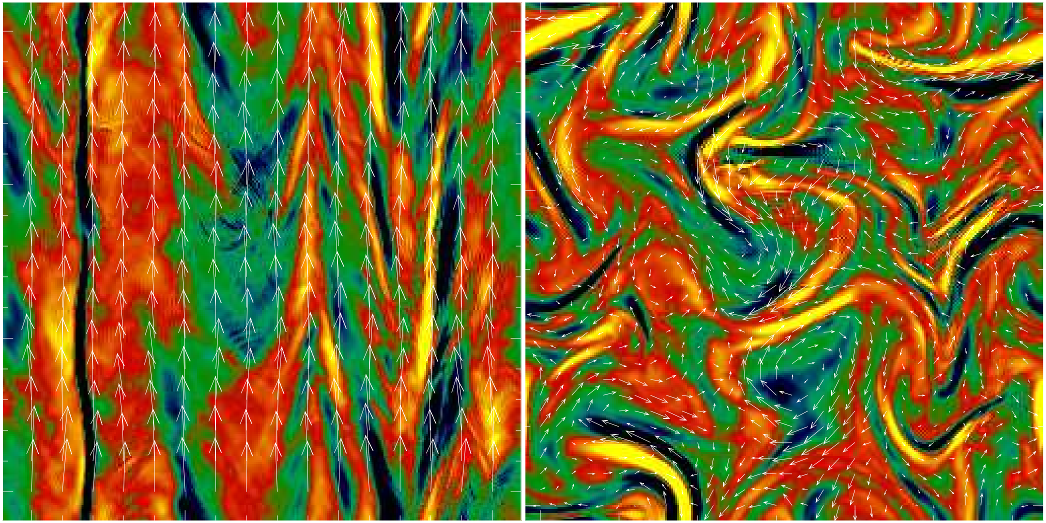

xz plane **xy plane**

Particles

Equations of motion for charged particles:

$$\frac{d\mathbf{u}}{dt} = \frac{q}{m}(\frac{1}{c}\mathbf{u} \times \mathbf{B} + \mathbf{E}), \qquad \frac{d\mathbf{x}}{dt} = \mathbf{u}$$

Particles

Equations of motion for charged particles:

$$\frac{d\mathbf{u}}{dt} = \frac{q}{m}(\frac{1}{c}\mathbf{u} \times \mathbf{B} + \mathbf{E}), \qquad \frac{d\mathbf{x}}{dt} = \mathbf{u}$$

with electric field

$$\mathbf{E} = -\frac{1}{c}\mathbf{v} \times \mathbf{B} + \frac{v_0 L}{R_m c}\mathbf{J} = \text{inductive } + \text{ resistive}$$

Particles

Equations of motion for charged particles:

$$\frac{d\mathbf{u}}{dt} = \frac{q}{m}(\frac{1}{c}\mathbf{u} \times \mathbf{B} + \mathbf{E}), \qquad \frac{d\mathbf{x}}{dt} = \mathbf{u}$$

with electric field

$$\mathbf{E} = -\frac{1}{c}\mathbf{v} \times \mathbf{B} + \frac{v_0 L}{R_m c}\mathbf{J} = \text{inductive } + \text{ resistive}$$

Particle gyrofrequency $w_g = qB/(mc) \rightarrow$ (small) lengthscale $r_g = u_\perp/w_g = u_\perp mc/(qB)$.
If $u_\perp = v_0$, $B = B_0 \rightarrow$ gyroradius $r_0 = v_0 mc/(qB_0)$.

Turbulent length scales vs particle scales

Dissipation length $l_d \approx \rho_{ii}$ (ion skin depth)

Supported by solar wind observations, linear Vlasov theory, kinetic physics reconnection studies.

$$\rho_{ii} = \text{ion skin depth} = c/w_{pi} = c/\sqrt{e^2 4\pi n/m_p}$$

Turbulent length scales vs particle scales

Dissipation length $l_d \approx \rho_{ii}$ (ion skin depth)

Supported by solar wind observations, linear Vlasov theory, kinetic physics reconnection studies.

$$\rho_{ii} = \text{ion skin depth} = c/w_{pi} = c/\sqrt{e^2 4\pi n/m_p}$$

$\rho_{ii}/L \ll 1$ for astrophysical and space plasmas ($\rho_{ii}/L \approx 10^{-5}$ for solar wind)

Turbulent length scales vs particle scales

Dissipation length $l_d \approx \rho_{ii}$ (ion skin depth)

Supported by solar wind observations, linear Vlasov theory, kinetic physics reconnection studies.

$$\rho_{ii} = \text{ion skin depth} = c/w_{pi} = c/\sqrt{e^2 4\pi n/m_p}$$

$\rho_{ii}/L \ll 1$ for astrophysical and space plasmas ($\rho_{ii}/L \approx 10^{-5}$ for solar wind)

We consider $\rho_{ii}/L = 1/32, \quad L_{box} \approx 200\rho_{ii}$

Turbulent length scales vs particle scales

Dissipation length $l_d \approx \rho_{ii}$ (ion skin depth)

Supported by solar wind observations, linear Vlasov theory, kinetic physics reconnection studies.

$$\rho_{ii} = \text{ion skin depth} = c/w_{pi} = c/\sqrt{e^2 4\pi n/m_p}$$

$\rho_{ii}/L \ll 1$ for astrophysical and space plasmas ($\rho_{ii}/L \approx 10^{-5}$ for solar wind)

We consider $\rho_{ii}/L = 1/32, \quad L_{box} \approx 200\rho_{ii}$

Particle (nominal) gyroradius vs turbulent dissipative scale

$$\frac{r_0}{l_d} = Z\frac{m}{m_p}\frac{\delta B}{B_0}$$

electrons $\rightarrow r_0^e/l_d = 6 \times 10^{-5}$

protons $\rightarrow r_0^p/l_d = 0.1$

Electrons (rms displacement)

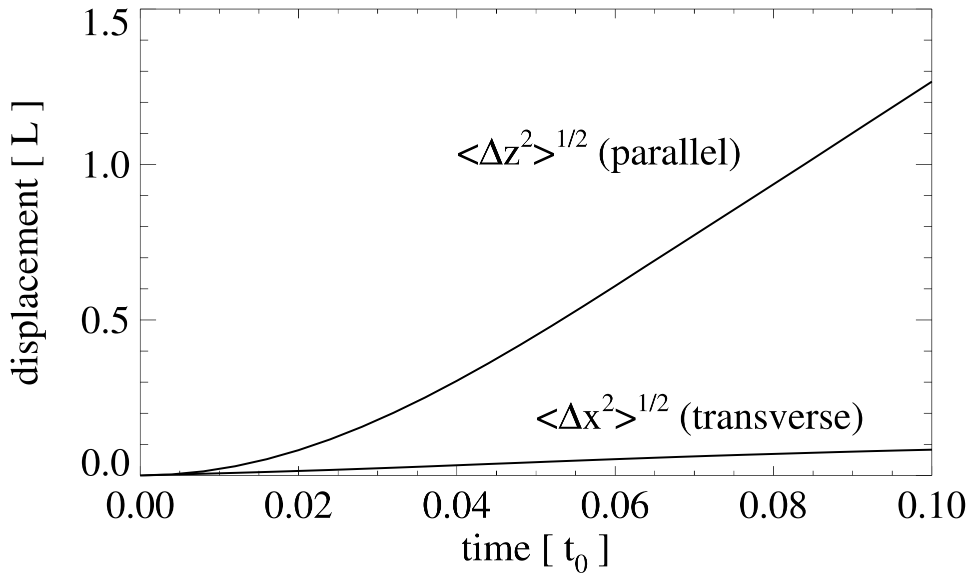

Run stops when $<\Delta z^2>^{1/2} \approx L$

Electrons (rms velocity)

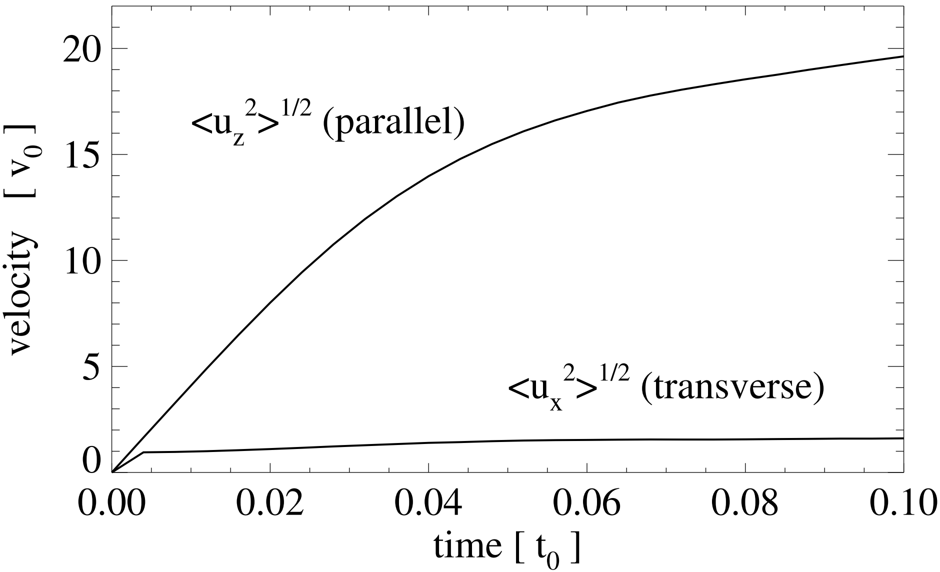

Electrons (parallel/transverse velocity square)

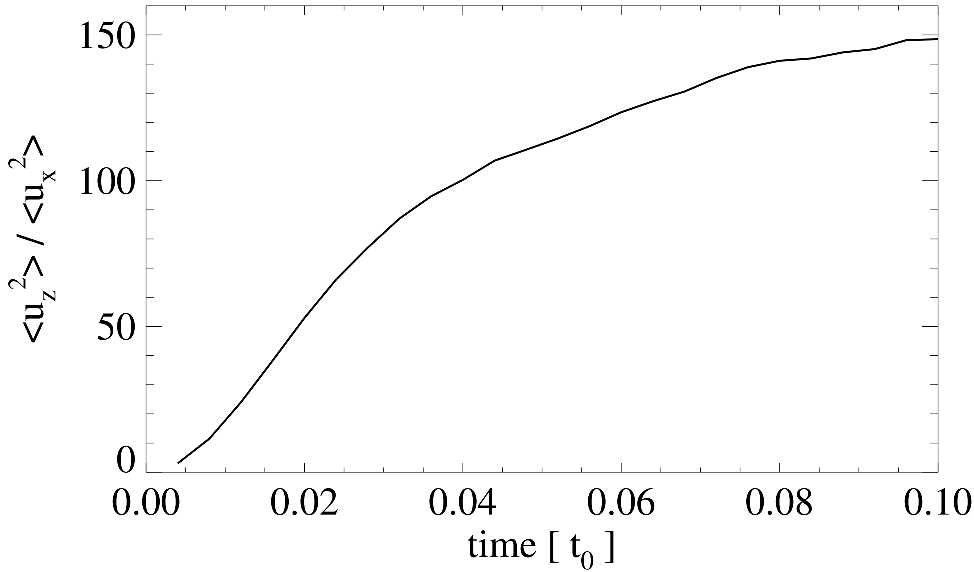

$T^e_{\parallel} \gg T^e_{\perp}$

Electrons (velocity distribution)

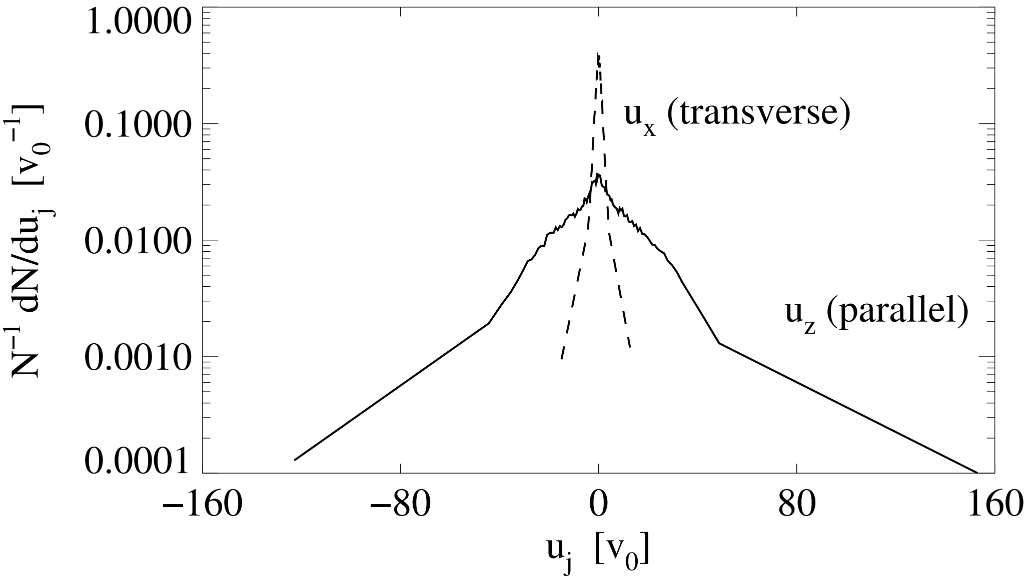

In $t = 10^4 \tau_e = 0.1 t_0$ with $\tau_e = 2\pi m_e c/(eB_0)$

Electrons (velocity scatter plot)

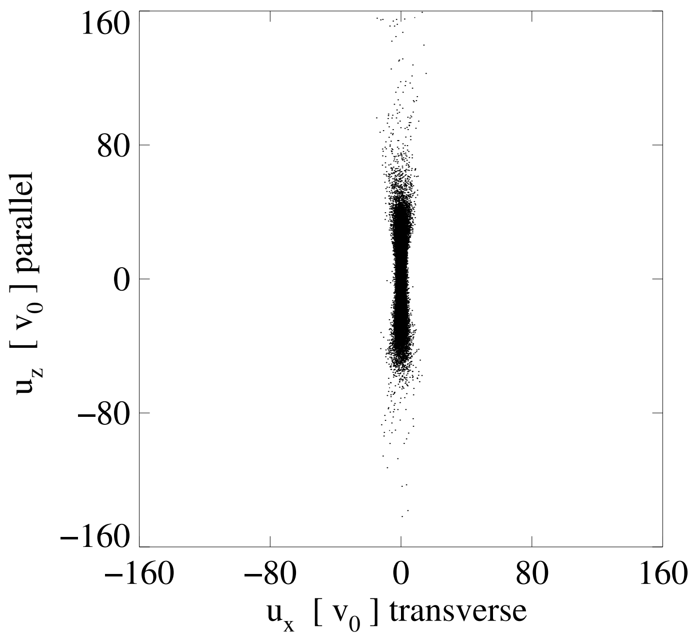

Electrons (gyroradii)

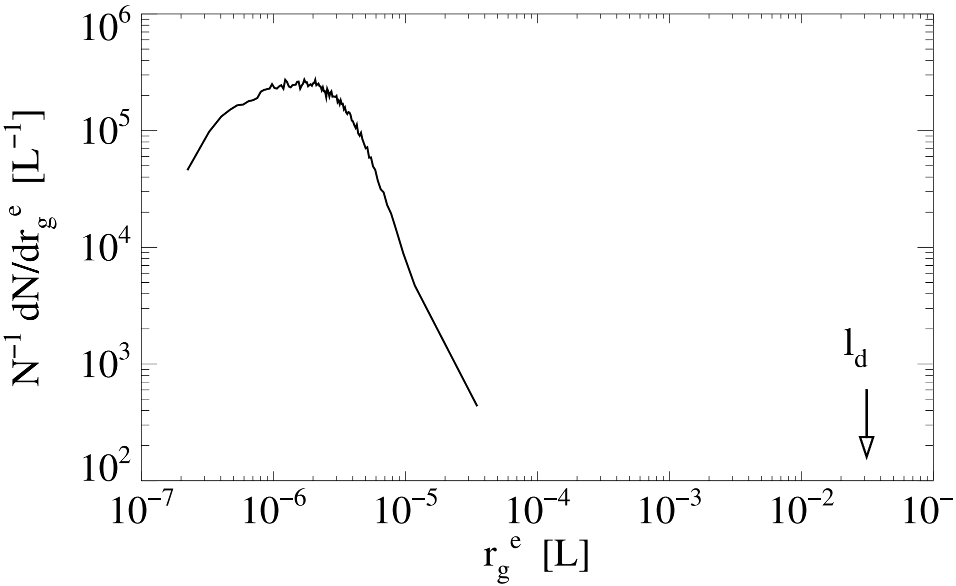

$$r_g^e = u_\perp m_e c/(eB_0)$$

Electrons (trajectories)

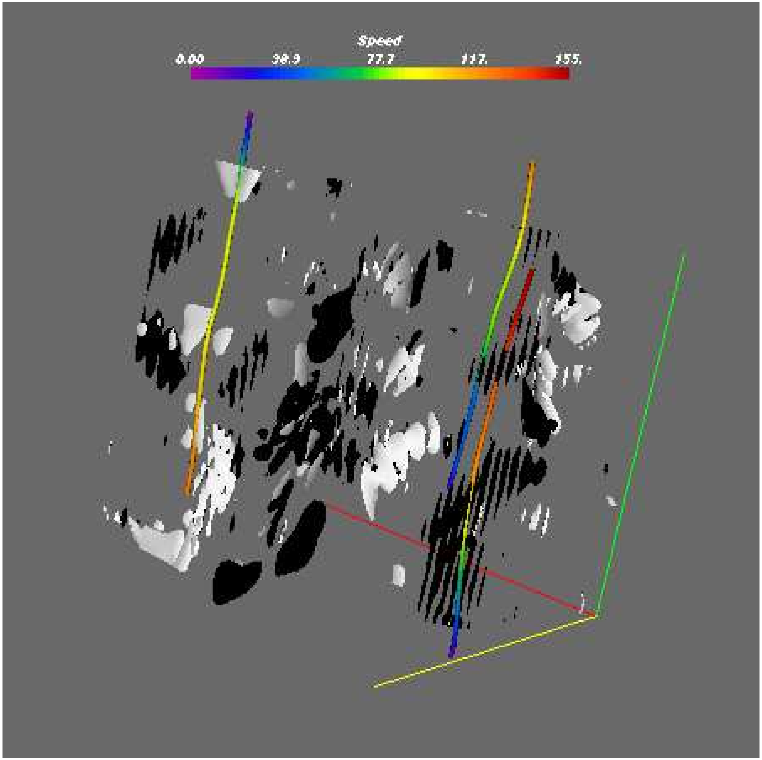

Electron parallel velocity gain: scaling

$$\frac{d\mathbf{u}_\parallel}{dt} = -\frac{e}{m_e}\mathbf{E}_\parallel = -\frac{e}{m_e c}\frac{v_0 L}{R_m}\mathbf{J}_\parallel, \qquad \frac{dz}{dt} = u_\parallel$$

Electron parallel velocity gain: scaling

$$\frac{d\mathbf{u}_\parallel}{dt} = -\frac{e}{m_e}\mathbf{E}_\parallel = -\frac{e}{m_e c}\frac{v_0 L}{R_m}\mathbf{J}_\parallel, \qquad \frac{dz}{dt} = u_\parallel$$

$$\Delta z \approx L \text{ in } t = t_\parallel = (2m_e c R_m/eu_0 J_\parallel)^{1/2} \rightarrow \Delta u_\parallel = (2eu_0 J_\parallel/m_e c R_m)^{1/2} L$$

Electron parallel velocity gain: scaling

$$\frac{d\mathbf{u}_\parallel}{dt} = -\frac{e}{m_e}\mathbf{E}_\parallel = -\frac{e}{m_e c}\frac{v_0 L}{R_m}\mathbf{J}_\parallel, \qquad \frac{dz}{dt} = u_\parallel$$

$$\Delta z \approx L \text{ in } t = t_\parallel = (2m_e c R_m / e u_0 J_\parallel)^{1/2} \rightarrow \Delta u_\parallel = (2 e u_0 J_\parallel / m_e c R_m)^{1/2} L$$

which can be rewritten using $J_0 = \delta B/L$ and ρ_{ii} as

$$\Delta u_\parallel = [\ \frac{2m_p}{m_e}\frac{L}{\rho_{ii}}\frac{1}{R_m}\frac{J_\parallel}{J_0}\ ]^{1/2} v_0$$

Electron parallel velocity gain: scaling

$$\frac{d\mathbf{u}_{\parallel}}{dt} = -\frac{e}{m_e}\mathbf{E}_{\parallel} = -\frac{e}{m_e c}\frac{v_0 L}{R_m}\mathbf{J}_{\parallel}, \qquad \frac{dz}{dt} = u_{\parallel}$$

$\Delta z \approx L$ in $t = t_{\parallel} = (2m_e c R_m / e u_0 J_{\parallel})^{1/2} \rightarrow \Delta u_{\parallel} = (2 e u_0 J_{\parallel} / m_e c R_m)^{1/2} L$

which can be rewritten using $J_0 = \delta B / L$ and ρ_{ii} as

$$\Delta u_{\parallel} = [\ \frac{2m_p}{m_e}\frac{L}{\rho_{ii}}\frac{1}{R_m}\frac{J_{\parallel}}{J_0}\ ]^{1/2} v_0$$

Using $J_{\parallel}^{max}/J_0 = 47$ we get $t_{\parallel} \approx 0.03 t_0$ and $\Delta u_{\parallel} \approx 74 v_0$ for the maximum velocity

Electron parallel velocity gain: scaling

$$\frac{d\mathbf{u}_\parallel}{dt} = -\frac{e}{m_e}\mathbf{E}_\parallel = -\frac{e}{m_e c}\frac{v_0 L}{R_m}\mathbf{J}_\parallel, \qquad \frac{dz}{dt} = u_\parallel$$

$\Delta z \approx L$ in $t = t_\parallel = (2m_e c R_m / e u_0 J_\parallel)^{1/2} \rightarrow \Delta u_\parallel = (2 e u_0 J_\parallel / m_e c R_m)^{1/2} L$

which can be rewritten using $J_0 = \delta B/L$ and ρ_{ii} as

$$\Delta u_\parallel = [\ \frac{2m_p}{m_e}\frac{L}{\rho_{ii}}\frac{1}{R_m}\frac{J_\parallel}{J_0}\ ]^{1/2} v_0$$

Using $J_\parallel^{max}/J_0 = 47$ we get $t_\parallel \approx 0.03 t_0$ and $\Delta u_\parallel \approx 74 v_0$ for the maximum velocity

Using $\bar{J}_\parallel/J_0 = 4.5$ we get $t_\parallel \approx 0.09 t_0$ and $\Delta u_\parallel \approx 20 v_0$ for the average velocity

Protons (mean square velocities)

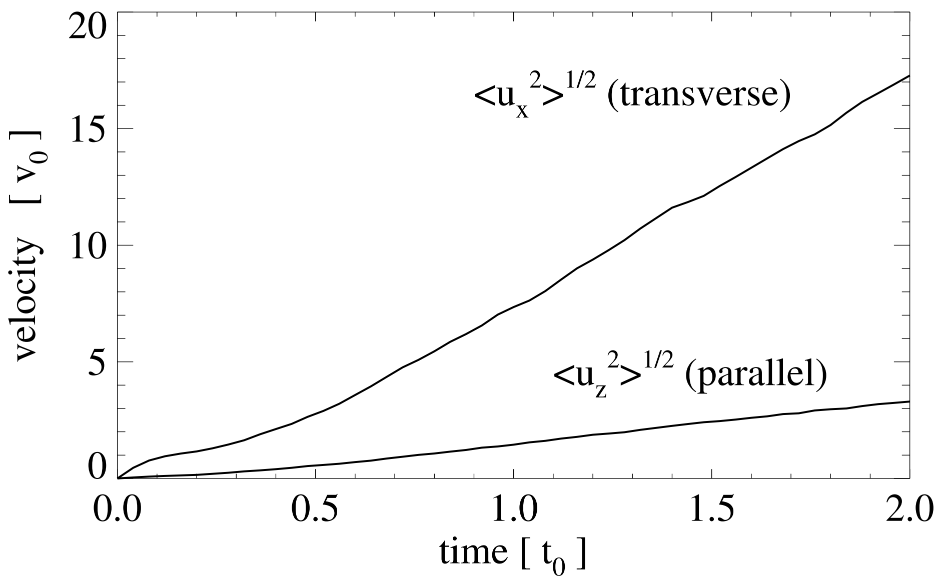

$T^i_\perp \gg T^i_\parallel$

Protons (velocity distribution function)

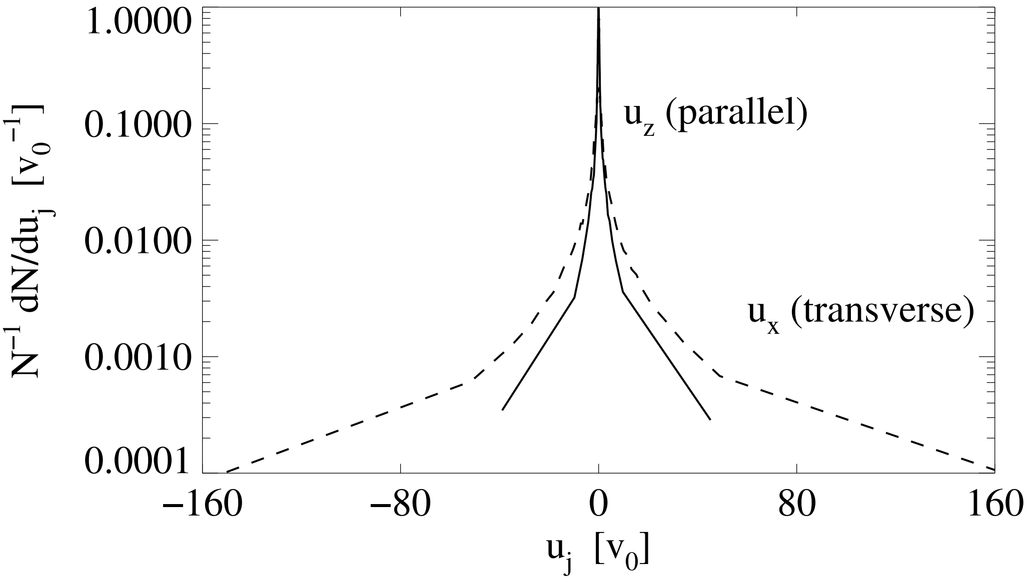

At $t = 90\tau_p = 1.8t_0$ with $\tau_p = 2\pi m_p c/(eB_0)$

Protons (velocity scatter plot)

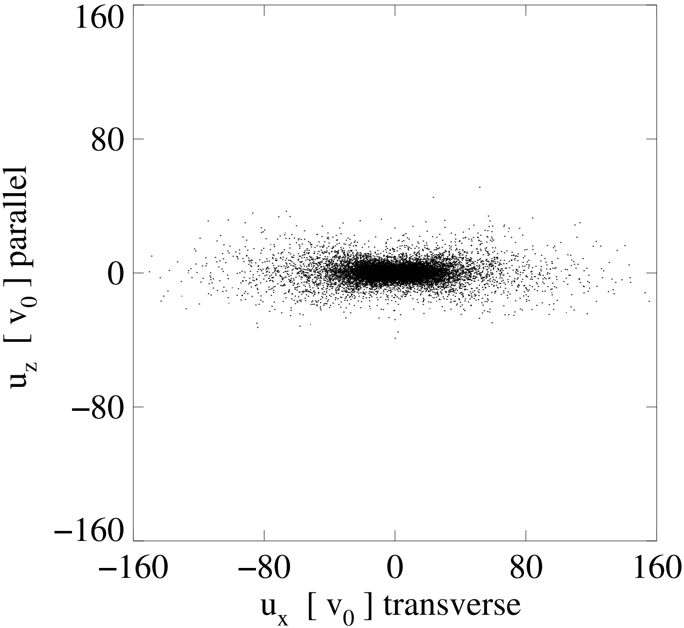

Protons: gyroradii at $t = 2\tau_p = 0.04 t_0$

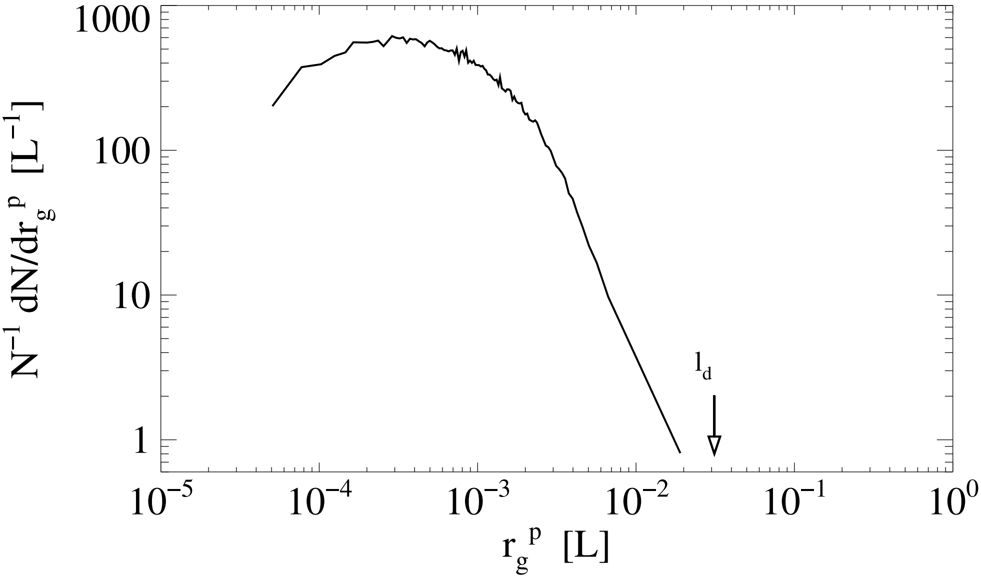

$$r_g^p = u_\perp m_p c/(eB_0)$$

Protons: gyroradii at $t = 20\tau_p = 0.4t_0$

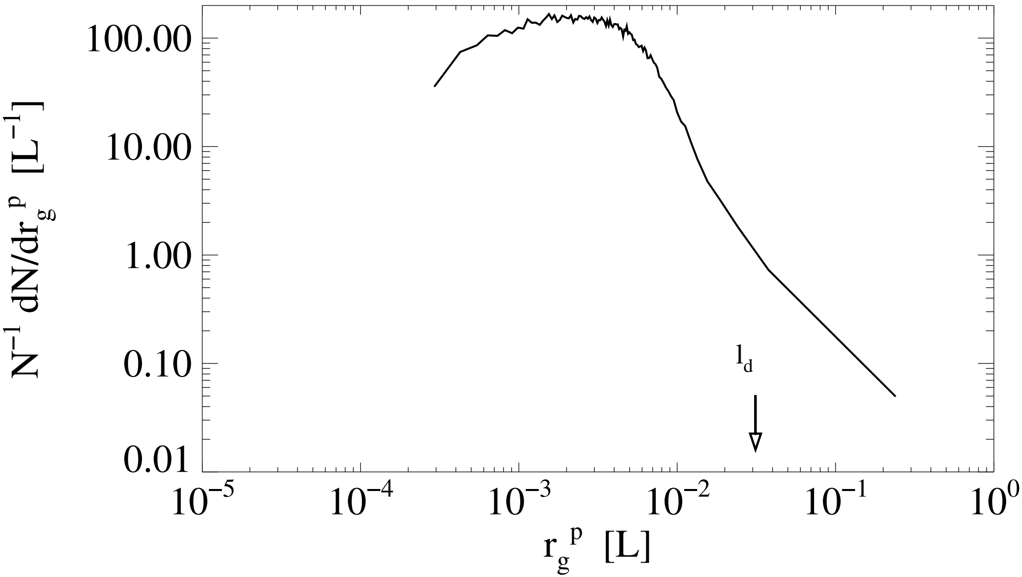

Protons: gyroradii at $t = 90\tau_p = 1.8t_0$

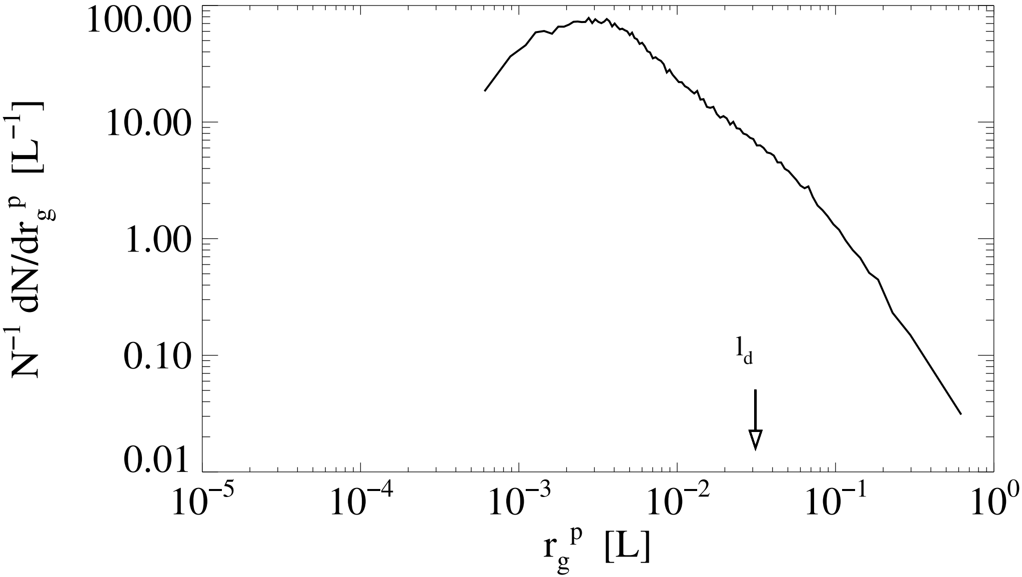

Protons: trajectories

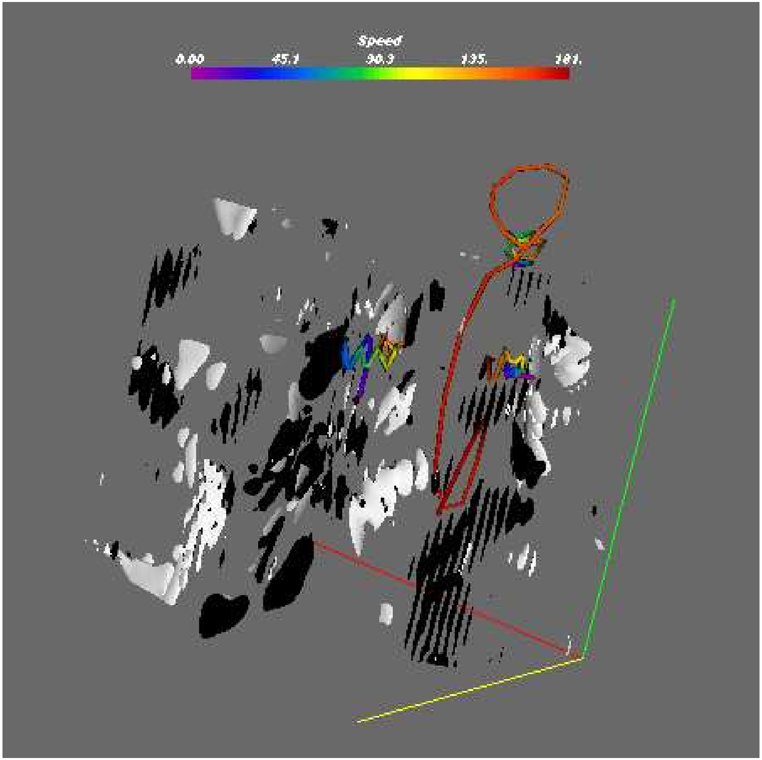

Protons: trajectories top view

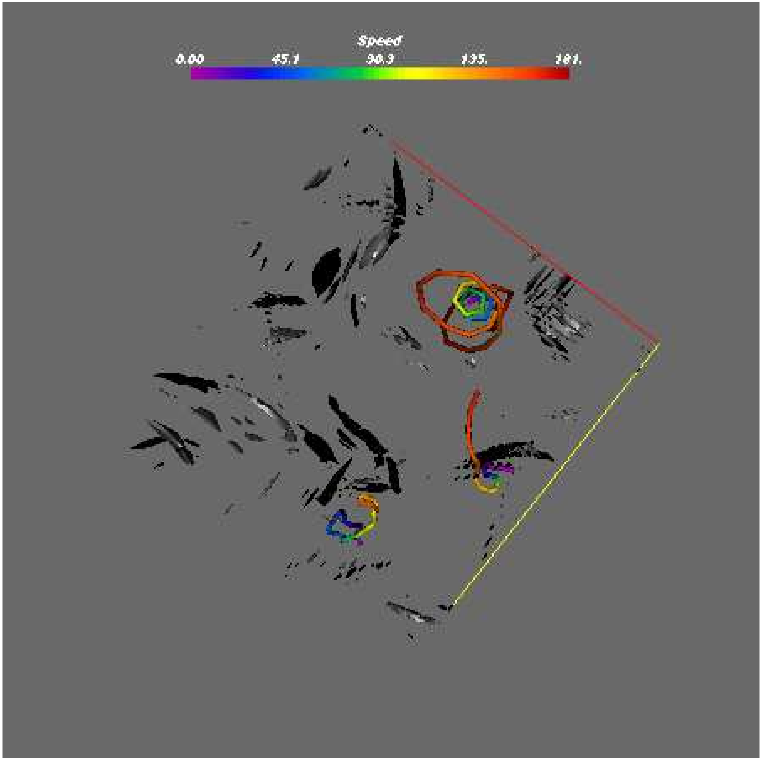

Proton transverse velocity gain: scaling

In the gyromotion $u_\perp = w_p r$, with $w_p = eB_0/(m_p c)$ or equivalently $u_\perp / v_0 = (B_0/\delta B)(r/\rho_{ii})$.

Proton transverse velocity gain: scaling

In the gyromotion $u_\perp = w_p r$, with $w_p = eB_0/(m_p c)$ or equivalently $u_\perp/v_0 = (B_0/\delta B)(r/\rho_{ii})$.

Energy gain stops at a critical gyroradius r.

Proton transverse velocity gain: scaling

In the gyromotion $u_\perp = w_p r$, with $w_p = eB_0/(m_p c)$ or equivalently $u_\perp/v_0 = (B_0/\delta B)(r/\rho_{ii})$.

Energy gain stops at a critical gyroradius r. Estimating $r = \sqrt{L\rho_{ii}}$, we get

$$\frac{u_\perp}{v_0} \sim \frac{B_0}{\delta B}\left[\ \frac{L}{\rho_{ii}}\ \right]^{1/2}$$

Proton transverse velocity gain: scaling

In the gyromotion $u_\perp = w_p r$, with $w_p = eB_0/(m_p c)$ or equivalently $u_\perp/v_0 = (B_0/\delta B)(r/\rho_{ii})$.

Energy gain stops at a critical gyroradius r. Estimating $r = \sqrt{L\rho_{ii}}$, we get

$$\frac{u_\perp}{v_0} \sim \frac{B_0}{\delta B}\Big[\ \frac{L}{\rho_{ii}}\ \Big]^{1/2}$$

Using the numerical values $u_\perp \approx 60 v_0$

Effect of time dependent fields: just started, but...

Effect of time dependent fields: just started, but...

- Electrons move fast and with very small gyroradius, so, remain completely unaffected by the slow evolution of the MHD fields

Effect of time dependent fields: just started, but...

- Electrons move fast and with very small gyroradius, so, remain completely unaffected by the slow evolution of the MHD fields

- Ions are more sensitive to the time evolution of the MHD fields, (because they move slower and with larger gyroradius) resulting in slower energy gain, but still, we get large perp velocities in times of the order of the Alfven time. When $u_p >> v_A$ then the dynamics of the particles becomes unaffected by the slow time evolution of the fields.

Effect of time dependent fields: just started, but...

- Electrons move fast and with very small gyroradius, so, remain completely unaffected by the slow evolution of the MHD fields

- Ions are more sensitive to the time evolution of the MHD fields, (because they move slower and with larger gyroradius) resulting in slower energy gain, but still, we get large perp velocities in times of the order of the Alfven time. When $u_p >> v_A$ then the dynamics of the particles becomes unaffected by the slow time evolution of the fields.

- Another issue: influence of the Hall effect $\rightarrow$, negligible for electrons, it affects more (but not much) the behavior of ions (see Dmitruk & Matthaeus, Jour. Geophys. Res. 111, A12110, 2006)

Hall MHD turbulence

Electric field

$$\mathbf{E} = -\frac{\mathbf{v}}{c} \times \mathbf{B} + \frac{\mathbf{J} \times \mathbf{B}}{nec} + \eta \mathbf{J}$$

Hall MHD turbulence

Electric field

$$\mathbf{E} = -\frac{\mathbf{v}}{c} \times \mathbf{B} + \frac{\mathbf{J} \times \mathbf{B}}{nec} + \eta \mathbf{J}$$

Spectrum of the electric field

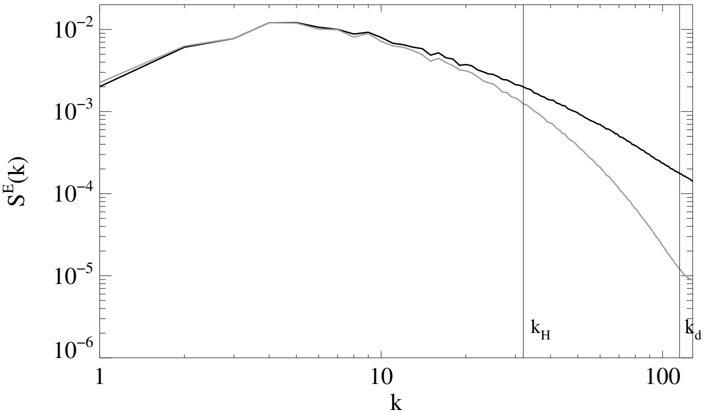

Distribution functions

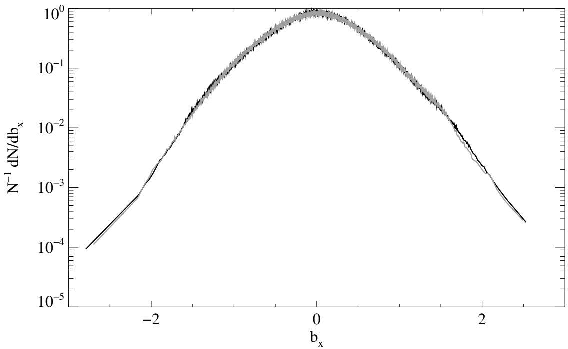

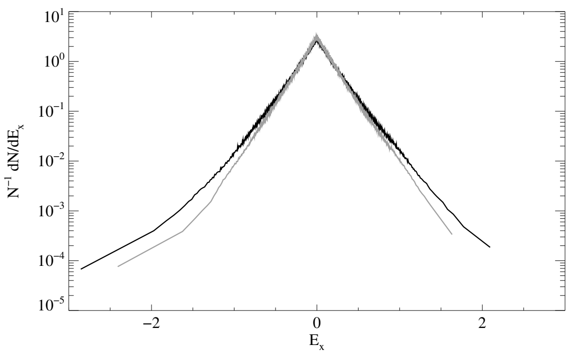

Effect on reconnection → changes the reconnection rate

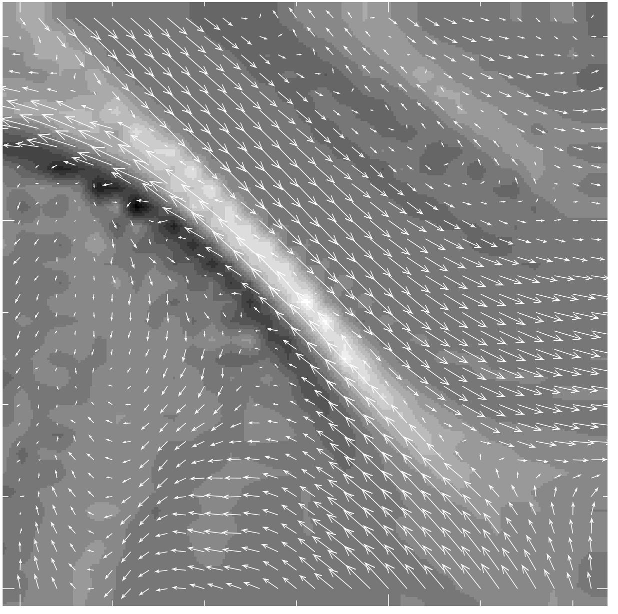

Dmitruk and Matthaeus, Phys. Plasmas 2006; also Reduced Hall MHD in Gomez, Dmitruk, Mahajan, Phys. Plasmas 2009; Martin, Dmitruk, Gomez, Phys. Plasmas 2010

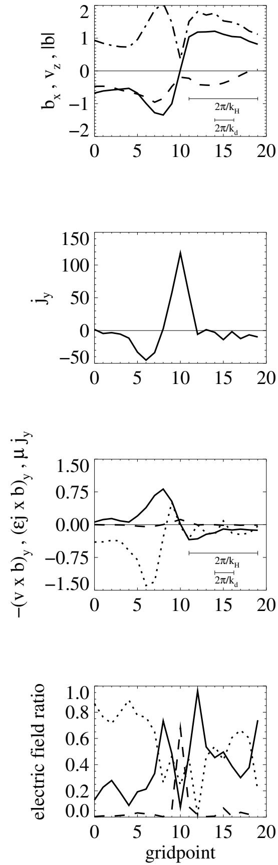

b_x , v_z , |b|
2π/k_H
2π/k_d
j_y
−(v x b)_y , (εj x b)_y , μ j_y
electric field ratio
gridpoint

Electrons (momentum distribution function)

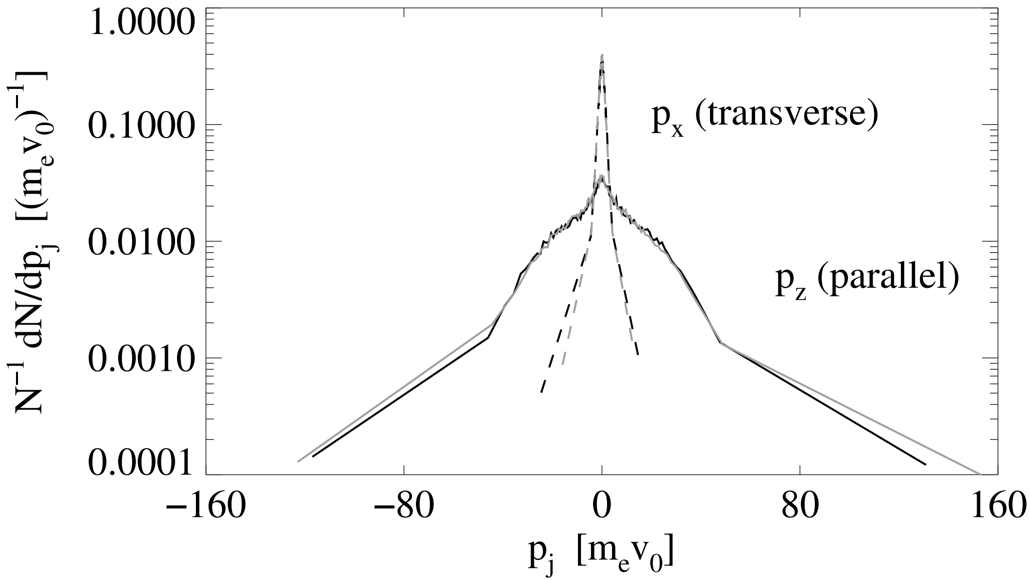

At $t = 10^4 \tau_e = 0.1 t_0$, for Hall and non-Hall (light lines)

Protons (momentum distribution function)

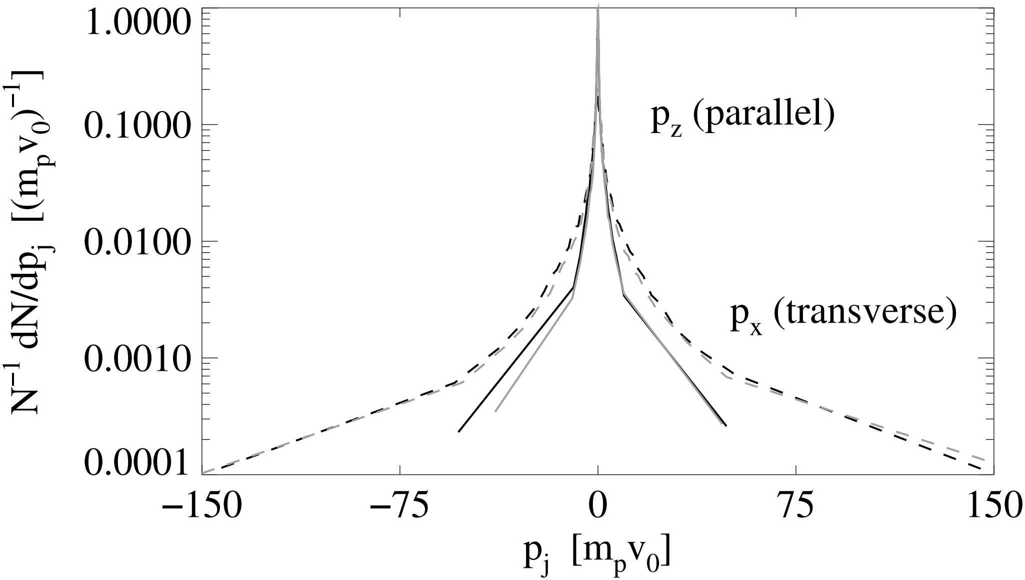

At $t = 90\tau_p = 1.8t_0$, for Hall and non-Hall (light lines)

Results with time dependent fields

Electrons (velocity distribution function)

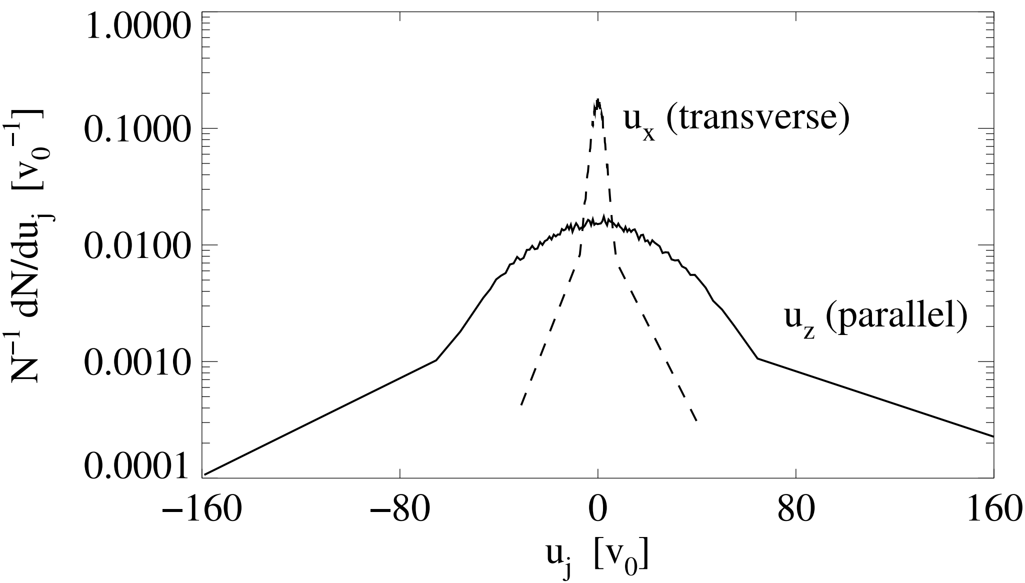

At $t = 10^4 \tau_e = 0.1 t_0$

Protons (velocity distribution function)

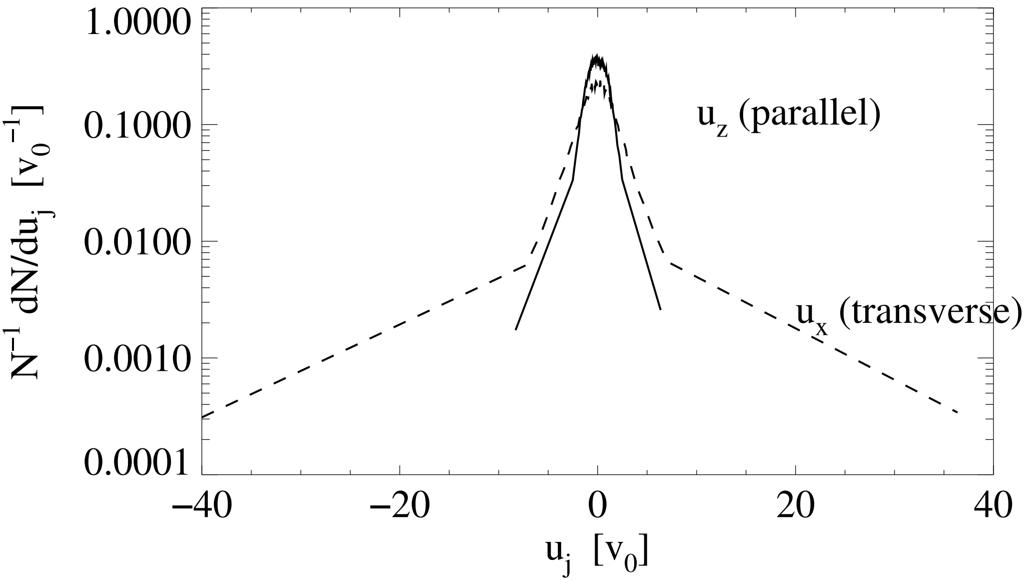

At $t = 200\tau_p = 4t_0$